APPENDIX D - Results of the 2018 bison and moose abundance survey for the proposed Tłı̨chǫ ASR

How to cite: Boulanger, J.B., Armstrong, T., Hodson, J., Cluff, D., and Kelly, A.P. 2024. Results of the 2018 bison and moose abundance survey for the proposed Tłı̨chǫ ASR. Government of the Northwest Territories, Department of Environment and Climate Change, Yellowknife, NT. September 2024.

Abstract

An aerial abundance survey of bison and moose was completed in February 2018, prior to the start of construction of the Tłı̨chǫ ASR, in accordance with the Tłı̨chǫ ASR WMMP. The survey was designed to use distance sampling methods to estimate the abundance of bison and moose in the study area. The 11,005 km^2 study area was centered on the proposed Tłı̨chǫ ASR alignment and surveyed between February 23 and March 2, 2018. The number of moose and bison observations from this survey alone were insufficient to reliably estimate a detection function for each species to estimate abundance. To obtain a sufficient sample size to estimate a detection function for each species, the 2018 Tłı̨chǫ ASR survey bison data was combined with data from a 2019 bison survey that used distance sampling methods, and the 2018 Tłı̨chǫ ASR moose survey data was combined with moose data from the 2021 NSR moose survey data and moose data collected during the 2019 Mackenzie bison survey, all from the same ecoregion. The 2018 bison abundance estimate for the Tłı̨chǫ ASR survey area, using a model averaged approach, was 197 bison (SE = 79.2, CI = 91-423, CV = 40%). There were no bison observed in the northern portion of the Tłı̨chǫ ASR survey area during the 2018 survey. Estimated across a smaller area (5,998 km^2) that better represented the northern extent of the Mackenzie bison range, the 2018 density of bison was 3.28 (SE = 1.32, CI = 1.52-7.05) bison per 100 km^2. The 2018 moose abundance estimate for the Tłı̨chǫ ASR area was 113 moose (SE = 28.7, CI = 69-185, CV = 0.25). The estimated density of moose across the 11,005 km^2 survey area was 1.03 moose per 100 km^2 (SE = 0.26, CI= 0.63-1.70). The 2021 moose abundance estimate for the Tłı̨chǫ ASR sub-area was 183 moose (SE = 50.6, CI = 106-316, CV = 0.28). The estimated density of moose across the 11,830 km2 survey area was 1.55 moose / 100 km2 (SE = 0.43, CI= 0.89-2.67). Although the 2021 moose estimate is higher than the 2018 estimate, there was no significant difference in the two estimates, given the moderate precision of the surveys (i.e., overlapping confidence intervals).

Introduction

Abundance surveys of bison and moose were required under the WMMP for the Tłı̨chǫ ASR[1]. To address potential changes in the relative abundance of bison and moose, the WMMP originally proposed late winter aerial surveys every three years to generate density estimates in the Tłı̨chǫ ASR: once before construction, once during construction, and every 3-5 years after the road opens. The objective of the 2018 survey was to obtain a baseline estimate of moose and bison density in the Tłı̨chǫ ASR regional study area prior to construction of the Tłı̨chǫ ASR. This survey was completed under wildlife research permit WL5005580. A wildlife research permit report was produced with

[1] https://www.gov.nt.ca/ecc/en/services/wildlife-management-and-monitoring-plans/wmmp-resources

preliminary results from this survey along with other fieldwork under the same permit (Hodson and Patenaude 2018).

Methods

Data Collection

We estimated abundance of bison and moose in the study area using distance sampling (Buckland et al. 2001). The 11,005 km^2 study area centered on the proposed Tłı̨chǫ ASR alignment (Figure D-1) with survey transect lines spaced 2 km apart. The survey was flown in a DHC-2 Beaver aircraft at a planned altitude of 150 m AGL and a planned speed of 90 knots (167 km/hr). The survey crew consisted of two observers, a navigator, and the pilot. The distance sampling method involves measuring the perpendicular distance of each moose or bison observation from the survey lines. When animals were spotted, the aircraft left the survey line to take a GPS location directly overhead of the animal or where it was first spotted if it moved before the aircraft arrived, and to make an accurate count. The canopy cover (none: less than 10% canopy cover; open: 10% - 50% forest canopy; closed: > 50% forest canopy) and vegetation type (conifer, deciduous, shrub, graminoid, grass, water) at the GPS location was also recorded. Large groups of animals were photographed to verify field counts. Perpendicular distances were measured from observation waypoints to the survey line using OziExplorer (© D & L Software Pty Ltd, www.oziexplorer.com) after the survey was completed.

Data Analysis

We used distance sampling methods (Buckland et al. 1993; Buckland et al. 2004; Thomas et al. 2009) to estimate density and abundance of bison and moose. In this method, the distribution of the number of observations made at different distances to survey transects is used to estimate a detection function to model how the probability of recording observations decreases as a function of distance from the line. The detection function is then used to estimate the density of moose or bison in the study area while accounting for decreasing likelihood of recording animals that are farther from the transect.

The number of bison and moose observations from this 2018 Tłı̨chǫ ASR survey alone were insufficient to estimate a detection function, as Buckland et al. (2001: 240) recommend at least 60 to 80 independent observations of a species to estimate a reliable detection function, and the February 2018 survey recorded 27 observations of bison (group sizes ranging from 1-54 bison), and 34 observations of moose (group sizes ranged from 1-3 animals). To obtain a sufficient sample size to estimate a detection function for bison, the 2018 Tlicho ASR survey data was combined with bison data from a 2019 Mackenzie bison survey that used distance sampling methods. Similarly, the 2018 Tłı̨chǫ ASR moose survey data was combined with moose data from the 2019 Mackenzie bison survey (that also recorded moose observations using distance sampling methods) and from the 2021 NSR moose survey from the same ecoregion. Figure D-2 (bison) and Figure D-13 (moose) show the overlap of these survey extents with the 2018 survey.

This procedure first involved screening the data to determine proper right and left truncation distances for the distance sampling data. In many cases animals directly under the plane are invisible

to observers, causing a "blind spot" in this area. The blind spot under the plane and the method of recording distances made it very likely that observations in the immediate area of the plane are underrepresented in the dataset. Distance methods assume that *sightability = 1* on the transect line and therefore inclusion of the full dataset would bias estimates. Therefore, the distribution of measured distances was initially screened, and data was left truncated to allow better estimation of sightability at the "shoulder" area where sightability should be close to one.

Data was also screened to determine if right truncation was required. Right truncation eliminates outlier observations that were at much further distances than most observations and therefore may overly influence model fitting.

Bison or moose that were observed while taking a GPS location over an observed group or searching off the transect line (secondary observations) were not included for the main analysis. Inclusion of these groups would bias estimates since detection functions are based upon observation distances relative to the plane and transect line. Therefore, the distance of secondary groups from the transect line did not correctly describe the sightability of these groups since they were not observed on the transect line.

Once data screening was completed, detection function models were fit to the data. The half-normal, and hazard rate detection functions were used to model reduction in sightability with distance. Covariates that also affected sightability were then modelled. Of most interest was the effect of survey area (Tłı̨chǫ ASR or Mackenzie), canopy cover (none, open, and closed) and group size on detection probabilities. Group size was entered as a covariate to allow assessment of the effect of group size in unison with other covariates. Information theoretic methods were used to compare candidate models (Burnham and Anderson 1992) and covariate predictions were assessed graphically to assess biological validity and model fit along with goodness of fit tests.

The *mark-recapture distance sampling* (MRDS) package (Laake et al. 2012) in program R (R Development Core Team 2023) was used to produce estimates for the survey strata (i.e., sub-areas) in the study area. Program MRDS uses newer variance estimation methods that allow estimates of variance when group size is a covariate (without bootstrapping) for survey strata (Innes et al. 2002; Buckland et al. 2004). Maps, graphs, and GIS files were produced using QGIS GIS software (QGIS Foundation 2020), *mapview* (Appelhans et al. 2023), *ggplot* (Wickham 2009), and simple features (*sf*) (Pebesma 2018) R packages.

Results

The Tłı̨chǫ ASR moose and bison survey was completed between February 23 and March 2, 2018. The survey took 47 hours and was flown on seven days. A total of 82 transects were flown. Weather and observing conditions ranged from poor to excellent with good to very good conditions most days. There was no flight on February 26 due to poor weather. The observers were Richard Romie of Whatì who flew each day, and GNWT-ECC Wildlife Division staff: Andrea Patenaude (three days), Heather Fenton (two days), Gabs Funwi (one day), and Robert Mulders (one day). Terry Armstrong (GNWT-ECC) was the navigator and data recorder, and Stephen Jeffery (Ahmic Air) was the pilot.

The February 2018 survey recorded 27 observations of bison, 34 observations of moose, and seven observations of boreal caribou, totalling 259 individuals across these three species (Table D-1). Five wolves were observed at a kill site. There were 33 transects without any wildlife or track observations (Figure D-1).

Table D-1. Wildlife observations recorded during a 2018 aerial survey for moose and bison within a 11,005 km^2 study area centered on the proposed Tłı̨chǫ ASR alignment.

Species	Number of observations	Range of group sizes (number of individuals)	Total number of individuals observed
Bison	27	1 – 54	174
Caribou	7	2 – 8	32
Moose	34	1 – 3	53
Wolf	1	5	5
Bison tracks	4	NA	NA
Caribou tracks	19	NA	NA
Old moose tracks	2	NA	NA

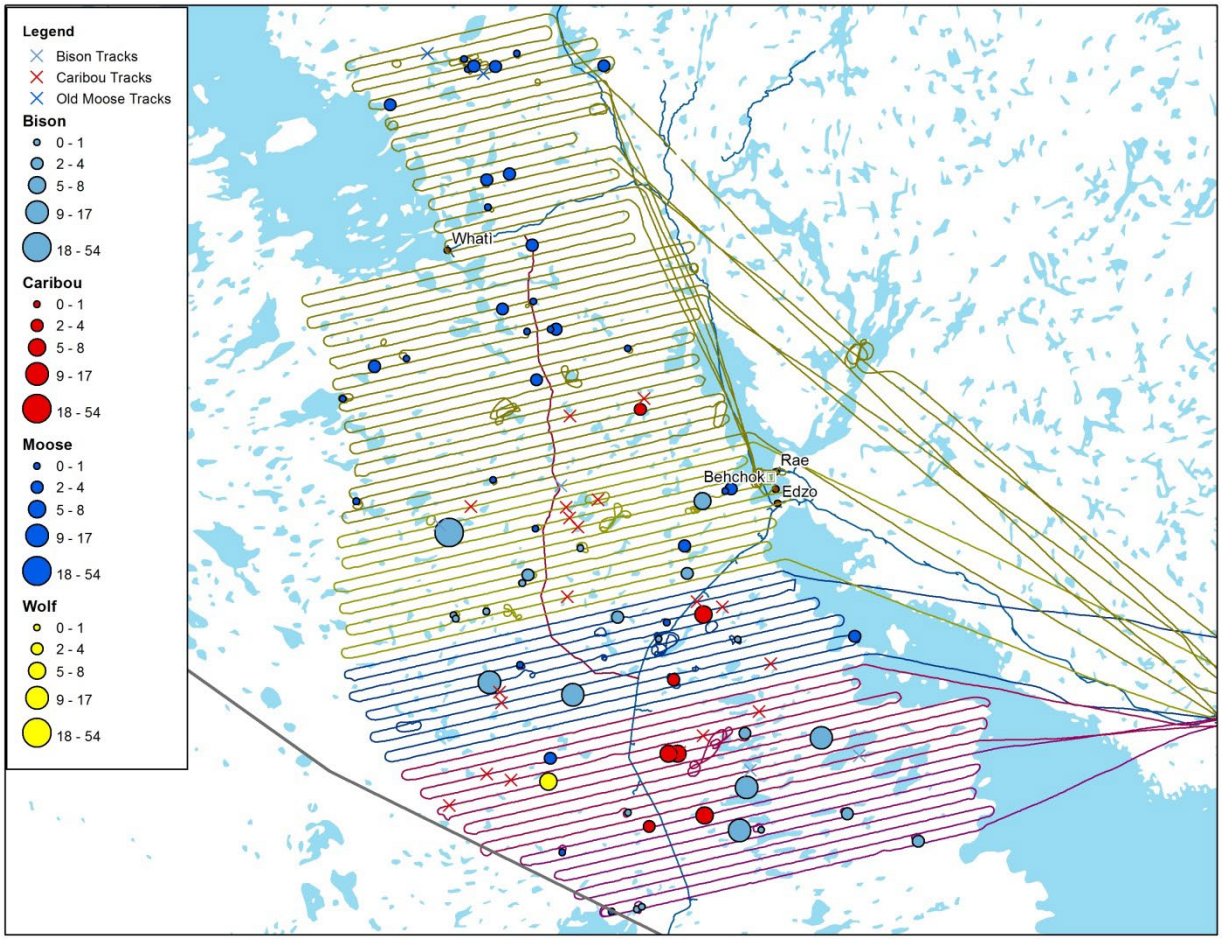

Figure D-1. Wildlife observations recorded during an aerial survey conducted within a 11,005 km^2 study area centered on the proposed Tłı̨chǫ ASR alignment between February 23 and March 2, 2018. Symbol sizes for each observation are proportional to the number of individuals in each group. Coloured lines represent the aerial survey transects flown, starting in the northern end of the study area working south.

Bison

Data Screening

Overall, 174 bison were observed in 27 groups during the 2018 Tłı̨chǫ ASR survey. Of these, one observation was secondary, meaning the bison were located when taking a GPS location of another bison or moose. This observation was eliminated (11 bison) and one observation was a duplicate. When these observations were filtered the total number of bison observed was 163 in 26 groups.

Data from the 2019 Mackenzie bison survey was added into the analysis to aid in modelling the detection function. The northern region of the Mackenzie survey overlapped the southern portion of the Tłı̨chǫ ASR survey (Figure D-2). Covariates were added to describe and model differences in detection functions and sample sizes due to overlap. First, *region* was used to define areas surveyed during the 2018 Tłı̨chǫ ASR survey (TASR), the Tłı̨chǫ ASR area surveyed during the 2019 Mackenzie survey (TASR-Mackenzie), and the Mackenzie area surveyed in 2019 that did not overlap with the Tłı̨chǫ ASR survey area (Mackenzie). Second, *zone* was defined that pertained to observations in the Tłı̨chǫ ASR or Mackenzie (area not overlapping with TASR) area regardless of what year they were surveyed. Finally, *project* (TASR or Mackenzie) was used to define the group (crew, aircraft, etc.) that did the actual survey.

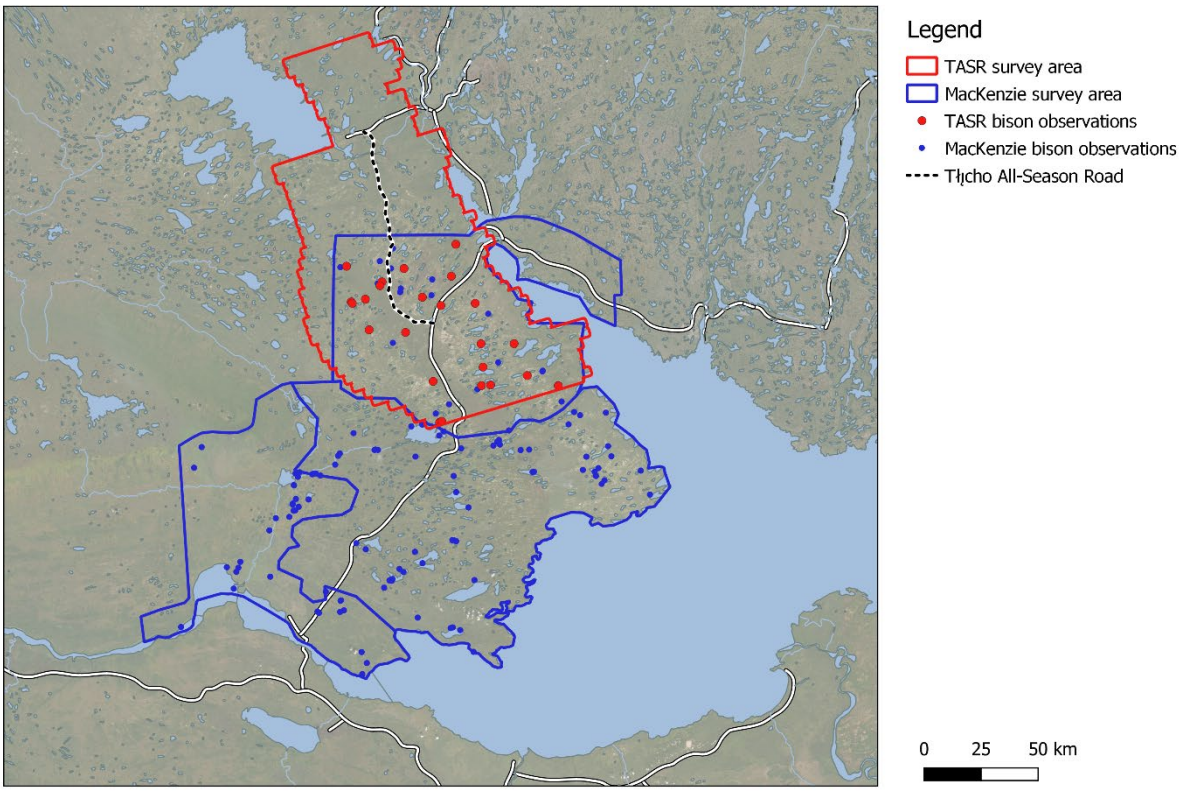

Figure D-2. Bison observations from the 2018 Tłı̨chǫ ASR (red) and 2019 Mackenzie bison survey (blue) used for the distance sampling analysis.

Left and right truncation values of 200 and 2,000 m were chosen based upon previous analyses of data from GNWT-ECC Mackenzie and Slave River bison abundance surveys. The 2,000 m right truncation was at the 97.5th percentile of observed distances of bison groups. The value of 200 m was also suggested by observation of histograms of distances (Figure D-3). Frequencies of observations closer to the plane were reduced substantially when observations within 200 m were included. This reduced the Tłı̨chǫ ASR dataset by 34 bison and three groups. No bison from the Tłı̨chǫ ASR dataset were eliminated by right truncation.

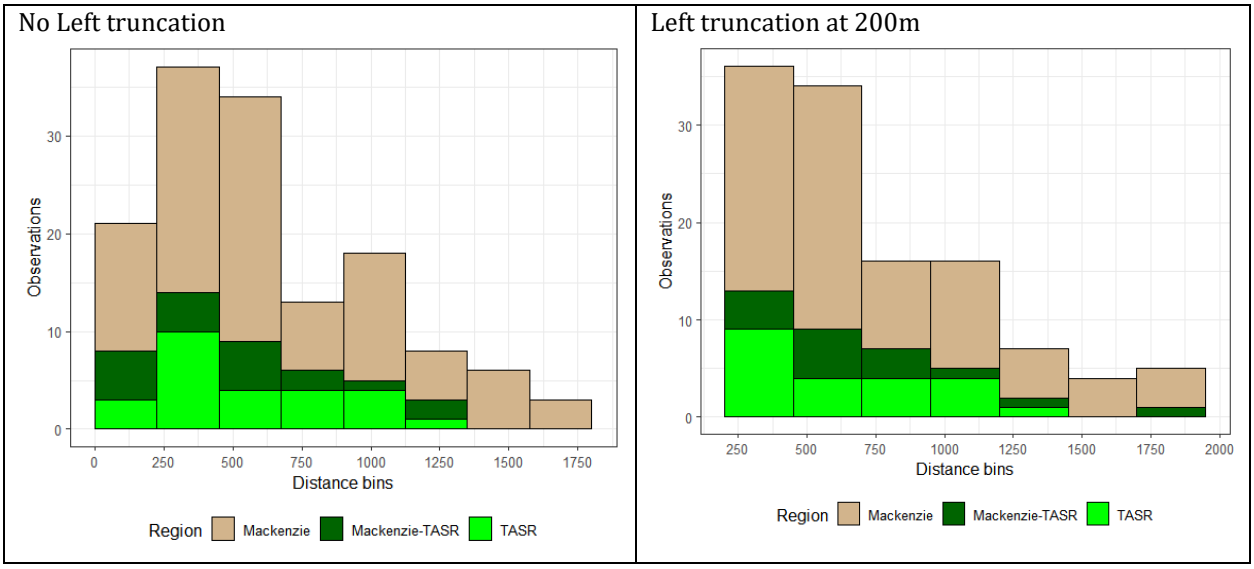

Figure D-3. Detection histograms without left truncation (left) and with the data left truncated at 200 m.

The range of group sizes for the Mackenzie and Tłı̨chǫ ASR areas were relatively similar, however, interpretation of ranges was challenged by low sample sizes in the Tłı̨chǫ ASR area. Five larger group sizes (>60 bison) were observed in the Mackenzie survey (Figure D-4). Given the likely effect of these group sizes on sightability, they were eliminated from the analysis therefore creating the same range of group sizes observed for Tłı̨chǫ ASR and Mackenzie surveys.

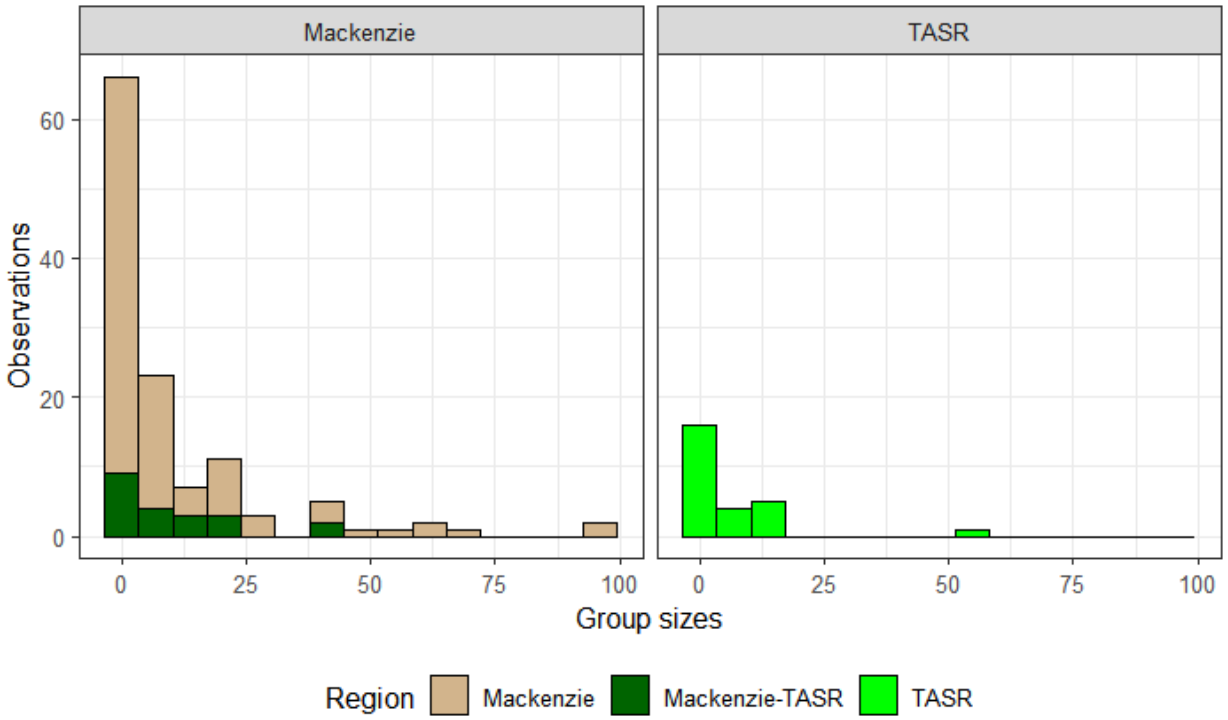

Figure D-4. Distributions of group sizes for the Mackenzie and Tłı̨chǫ ASR (TASR) studies as defined by regions of overlap.

A plot of group sizes by distance suggests a range of group sizes across all distances (Figure D-5). Correlation of the log of group size with distance suggests a non-significant relationship (Pearson ρ = 0.08, t = -.903, p = 0.369).

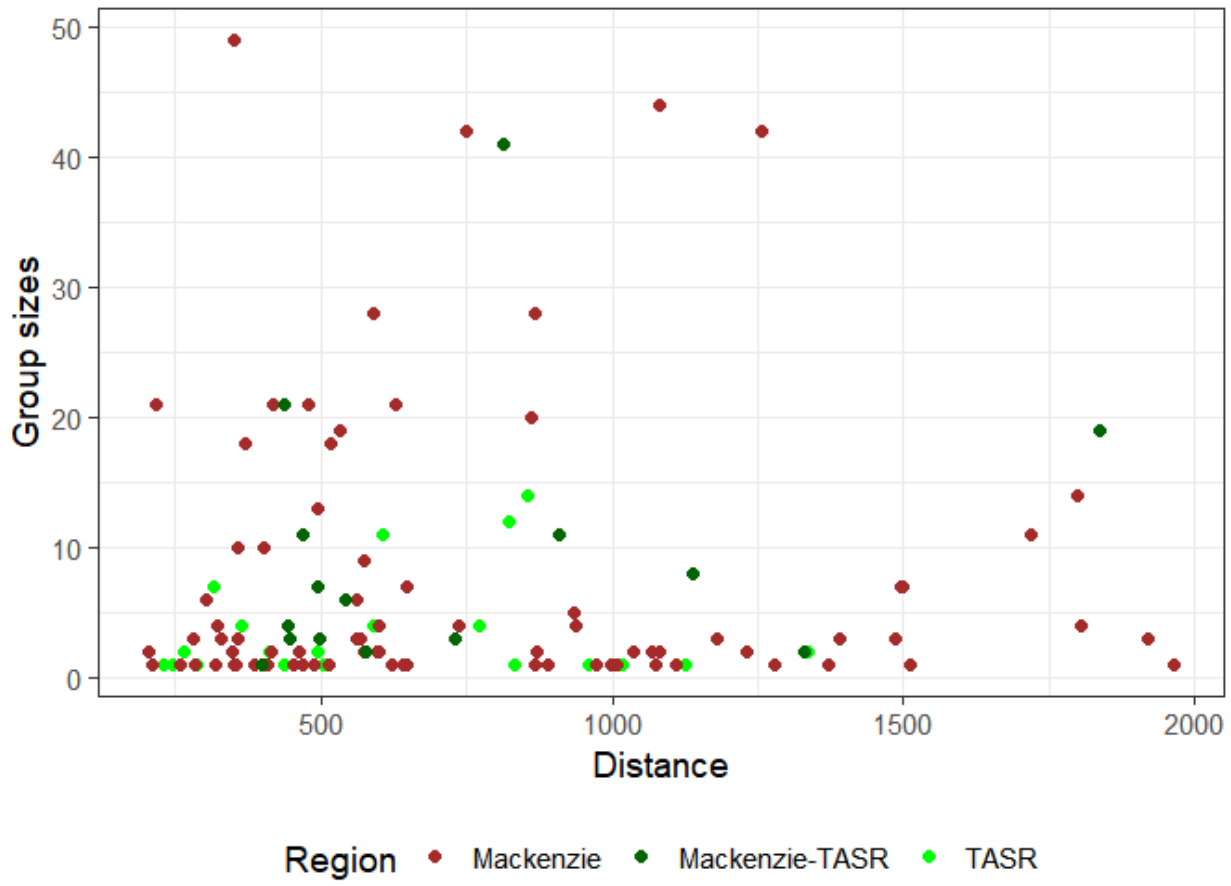

Figure D-5. Group sizes as a function of distance of observations by region.

Comparison of detection histograms by zone (area where survey occurred) suggests similar detection histograms. Region in this context refers to whether the Tłı̨chǫ ASR zone was surveyed during the 2018 Tłı̨chǫ ASR survey or the 2019 Mackenzie bison survey (Figure D-6).

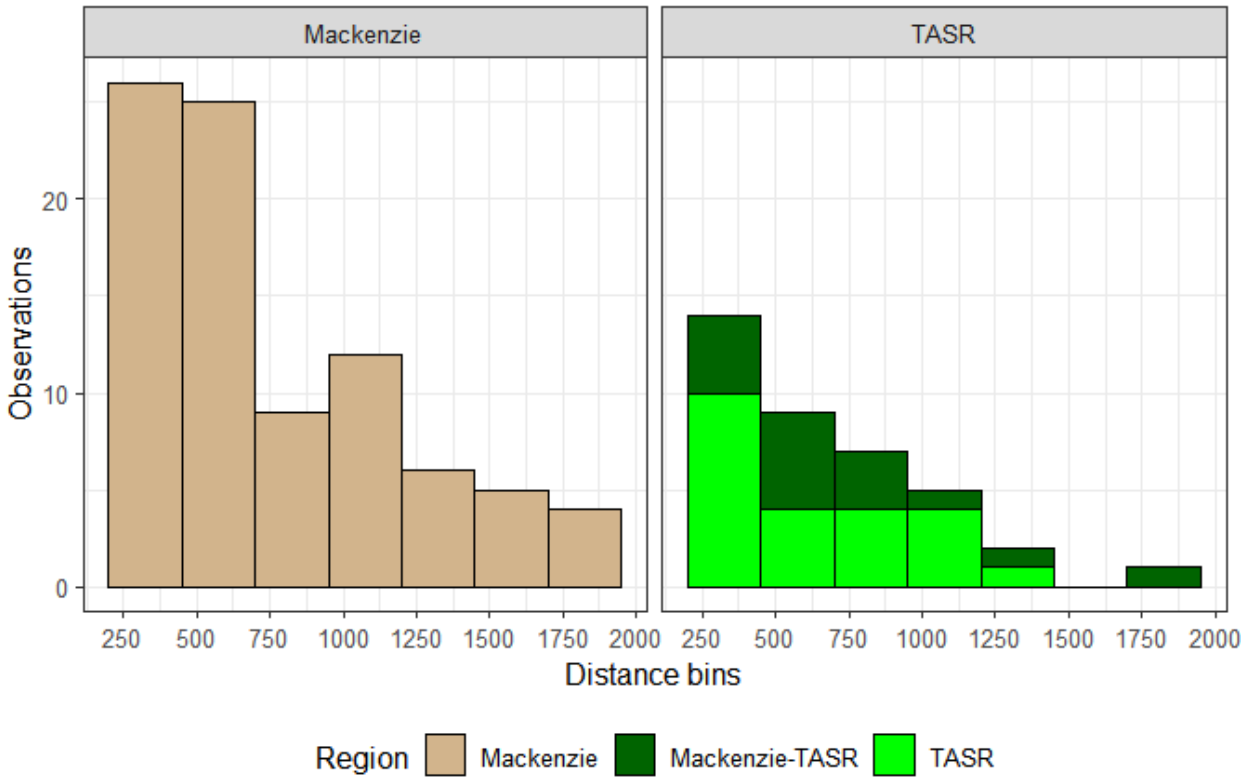

Figure D-6. Detection histograms by zone where the survey occurred. The zone (Mackenzie or TASR) shows the observations in the Mackenzie area not overlapping with TASR (left panel) or the observations from the TASR area (right panel) regardless of survey year. The coloured sub-bars in the right panel show the observations in 2018 from the TASR bison-moose survey (light green) and the 2019 observations from the 2019 Mackenzie bison survey (dark green).

Summaries of observations by canopy cover revealed only five groups observed in the closed canopy class. For this reason, closed (>50% canopy cover) and open canopy (which represent 10-50% canopy cover) were pooled. Observation of detection histograms suggests a wider range of distance for observations in the 'none' canopy class (i.e., 0% cover) compared to the closed-open class (Figure D-7).

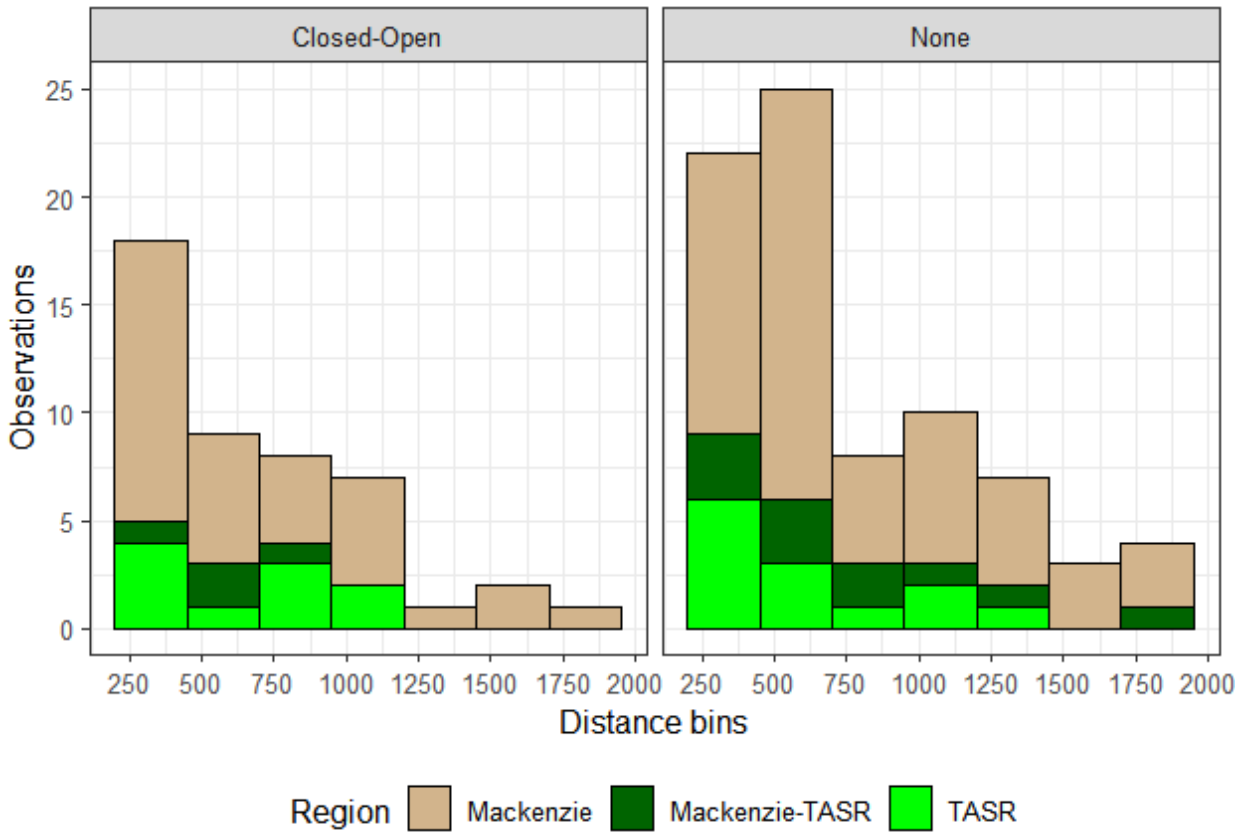

Figure D-7. Detection histograms by closed-open and no canopy cover classes.

Aircraft type can affect the probability of observers detecting animals close to the aircraft due to window placement, seat height, and other factors. A DHC-2 Beaver aircraft was used for the Tłı̨chǫ ASR survey whereas a Cessna 185 and Beaver aircraft were used for the 2019 Mackenzie bison survey. Comparison of detection histograms suggests more observations nearer to the plane for the Beaver, however, the range of distances of observations was similar (Figure D-8).

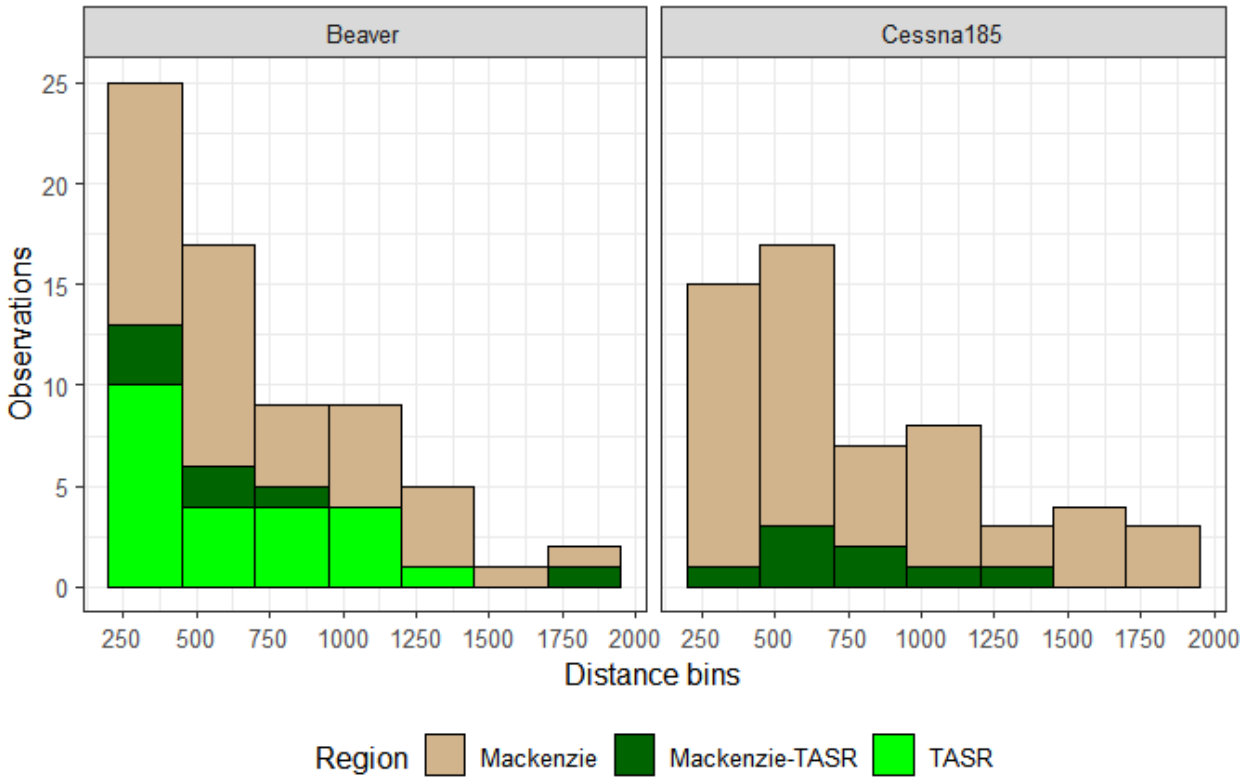

Figure D-8. Detection histograms for Beaver and Cessna aircraft used in the survey.

Table D-2 summarizes sample sizes used in the distance analysis. The Mackenzie study contributed 98 groups to the analysis of which 15 groups were within the Tłı̨chǫ ASR study area. Group sizes were relatively similar between each region.

Table D-2. Summary of bison data used for distance sampling analysis by region. The Mackenzie-Tłı̨chǫ ASR region is the area of overlap between the Tłı̨chǫ ASR and Mackenzie surveys surveyed in 2019 whereas Mackenzie refers to the 2019 survey area that did not overlap the Tłı̨chǫ ASR.

Region	Year	Left truncated (200 m)		Used in analysis						Right truncated (2,000 m)	
		Bison	Groups	Bison	Groups	Mean group size	SD	Min	Max	Bison	Groups
Mackenzie	2019	55	10	653	83	7.9	11.9	1	53	23	3
Mackenzie-Tłı̨chǫ ASR	2019	38	5	142	15	9.5	10.6	1	41	38	1
Tłı̨chǫ ASR	2018	34	3	129	23	5.6	11.2	1	54	0	0
Totals		127	18	924	121					61	4

Model Selection

Distance sampling models were then considered with a base half-normal and hazard rate detection function first applied to the dataset with a hazard rate detection function being most supported. However, covariates can affect the shape of detection functions and therefore the half-normal was also considered with other covariates. Covariates included project (2018 Tłı̨chǫ ASR survey or 2019 Mackenzie bison survey), zone (observations in the Tłı̨chǫ ASR or observations in the Mackenzie area (not overlapping with Tłı̨chǫ ASR) regardless of survey year), canopy cover, aircraft type and group size (size).

Of the covariates considered, canopy class was most supported with a half-normal detection function (Table D-3). No other covariates were more supported than the hazard rate model with a constant detection function. Estimates of abundance increased when project was added as a covariate. The increase in estimate with project was noteworthy; a topic explored further in sensitivity analyses to right truncation distance.

Many models were supported by the data as indicated by delta AICc values of less than 2. **A model averaged estimate based on all the models in Table D-3 was 197 bison (SE = 79.2, CI = 91-423, CV = 40%).** For model 1, 14% of the variance was due to estimation of detection probabilities and 86% was due to estimation of the encounter rate. This suggests that the main source of variation was the unequal distribution of bison in the survey area.

Table D-3. Model selection of distance covariate models for bison. Base detection functions (DF) are given for each model; 'hn' and 'hr' symbolize half-normal and hazard rate detection function models with 0 adjustment terms. 'Project' refers to project (2018 Tłı̨chǫ ASR survey or 2019 Mackenzie survey), 'zone' refers to whether sampling occurred in the Tłı̨chǫ ASR or in the Mackenzie sampling area outside of the Tłı̨chǫ ASR. 'Canopy' refers to canopy cover, 'size' refers to group size observed, and 'aircraft type' refers to aircraft used in the survey. Models with no covariates are termed 'constant'. AIC_c, the difference in AIC_c values between the ith model and the model with the lowest AIC_c value (ΔAICc), Akaike weights (w_i), number of parameters (K), and log-likelihood of the model are presented. Estimates for Tłı̨chǫ ASR (2018) are presented for each model.

No.	DF	Model	AICc	ΔAICc	w_i	K	LogL	N	SE	Conf. Limit		CV
1	hn	Canopy	1,749.03	0.00	0.11	2	-872.5	172	54.7	92	321	0.32
2	hn	Canopy + project	1,749.13	0.10	0.11	3	-871.5	224	85.9	107	468	0.38
3	hn	Zone + canopy	1,749.27	0.23	0.10	3	-871.5	206	72.2	104	406	0.35
4	hr	Constant	1,749.53	0.49	0.09	2	-872.7	172	60.0	87	339	0.35
5	hr	Canopy	1,749.57	0.54	0.09	3	-871.7	175	60.6	90	343	0.35
6	hn	Project	1,749.94	0.90	0.07	2	-872.9	236	90.5	113	493	0.38
7	hr	Project	1,750.36	1.32	0.06	3	-872.1	241	111.4	101	576	0.46
8	hn	Zone	1,751.00	1.96	0.04	2	-873.5	204	70.9	104	401	0.35
9	hr	Canopy + project	1,751.02	1.99	0.04	4	-871.4	227	104.7	95	541	0.46
10	hr	Zone	1,751.03	2.00	0.04	3	-872.4	194	77.6	90	417	0.40
11	hn	Constant	1,751.04	2.00	0.04	1	-874.5	169	55.1	89	320	0.33
12	hr	Aircraft type	1,751.35	2.31	0.04	3	-872.6	182	66.7	90	369	0.37
13	hn	Aircraft type	1,751.36	2.33	0.04	2	-873.6	188	63.1	98	362	0.34
14	hr	Zone + canopy	1,751.41	2.38	0.03	4	-871.6	191	76.9	88	412	0.40
15	hr	Size	1,751.47	2.43	0.03	3	-872.6	189	83.2	82	436	0.44
16	hr	Logsize	1,751.60	2.57	0.03	3	-872.7	170	63.9	82	350	0.38
17	hn	Size	1,752.87	3.84	0.02	2	-874.4	183	71.7	87	389	0.39
18	hn	Logsize	1,753.05	4.02	0.02	2	-874.5	165	55.3	86	317	0.34

The fit of model 1 was acceptable according to chi-square goodness of fit tests ($\chi^2 = 8.92$, df = 8, p = 0.34) and Cramer-Von Mises test (test statistic = 0.19, p = 0.27). A plot of the fit of the model to detection histograms also suggests adequate fit (Figure D-9).

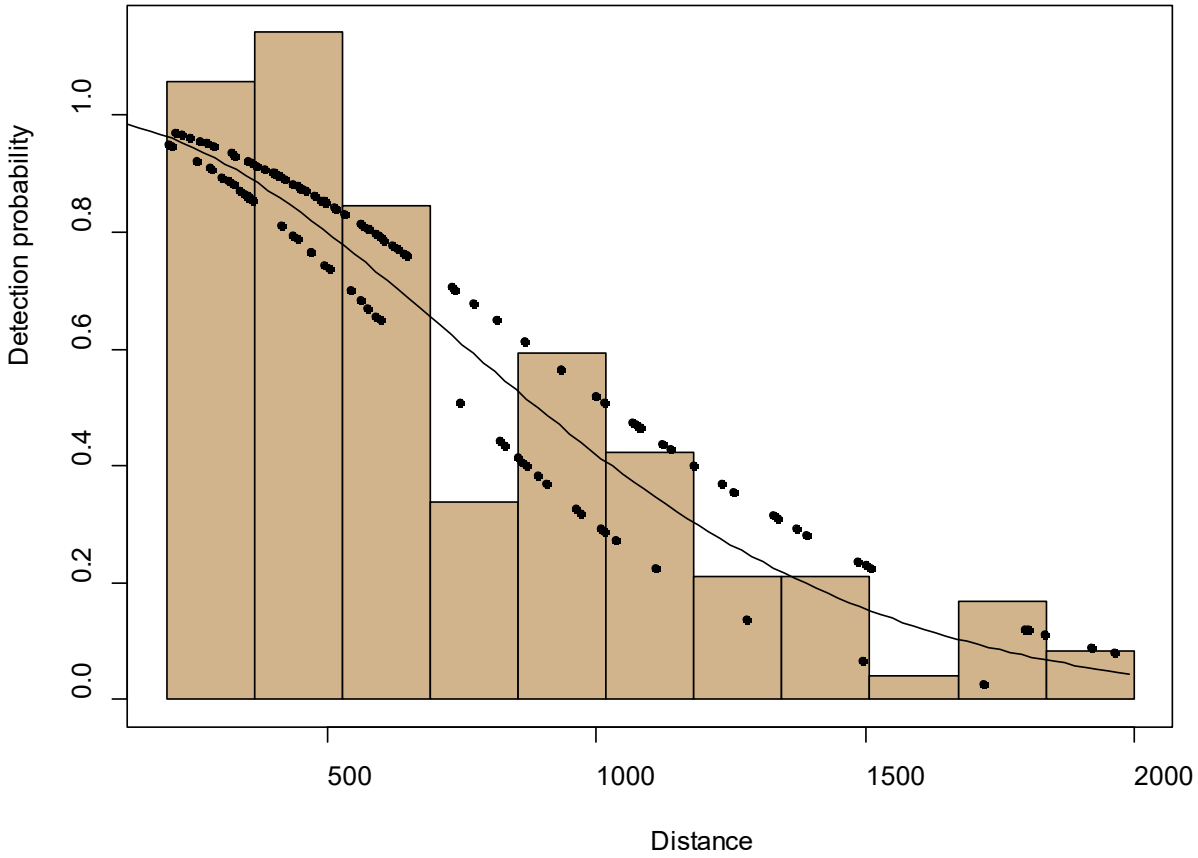

Figure D-9. Detection histograms and model estimates of the detection function for model 1 (HN:Canopy). The upper dotted line is the fit to the 'none' canopy category and the lower dotted line to the 'closed-open' canopy category.

Sensitivity Analyses

A sensitivity analysis of model 1 to left truncation distance revealed relative stability of estimates in the context of confidence limits. In general, estimates increased up to 150 m before plateauing at higher levels (Figure D-10).

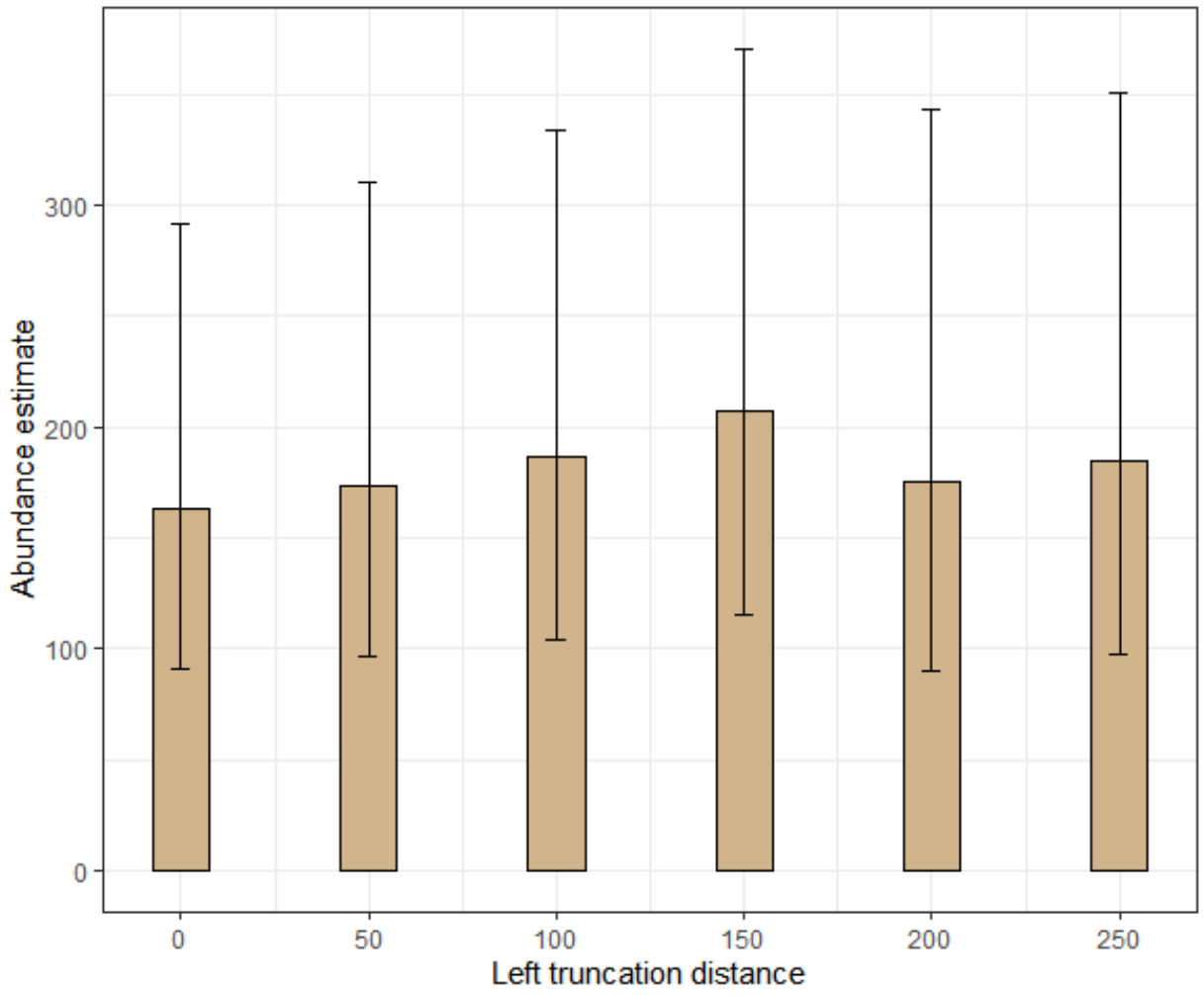

Figure D-10. Sensitivity of abundance estimates (error bars indicate 95% confidence limits) to left truncation distances.

Right truncation sensitivity was tested from the range used in most bison analyses (2,000 m) to the approximate range of distances in the 2018 Tłı̨chǫ ASR data set (1,500 m). Using the 1,500 m distance also tested sensitivity of the analysis to using a wider range of distances than the Tłı̨chǫ ASR survey for the analysis. This analysis was conducted for the full set of models considered in the analysis (Table D-3), which revealed sensitivity in model selection to the right truncation distances used. To confront this issue, we derived model averaged estimates from each right truncation distance analysis, which showed relative stability of estimates to right truncation distance used (Table D-4).

Table D-4. Model averaged estimates of abundance for the Tłı̨chǫ ASR area using different right truncation distances

Right truncation	Abundance	SE	Conf. limit		CV
2,000 m (used)	197	79.2	91	423	0.40
1,800 m	203	77.7	98	421	0.38
1,500 m (Tłı̨chǫ ASR distance range)	199	78.5	94	422	0.40

There were no bison observed in the northern portion of the Tłı̨chǫ ASR survey area during the 2018 survey (Figure D-1). Thus, the survey extent over which bison density was estimated was truncated by the north and west boundaries of the Mackenzie survey (Figure D-11). Density of bison was estimated across this smaller area (5,998 km^2), which is a more accurate delineation of the northern extent of the Mackenzie bison range as of 2018. The estimated density of bison in the truncated Tłı̨chǫ ASR area in 2018, using the model-averaged estimate of 197 bison (SE = 79.2, CI = 91-423, CV = 40%), is 3.28 bison (SE = 1.32, CI = 1.52-7.05) per 100 km^2.

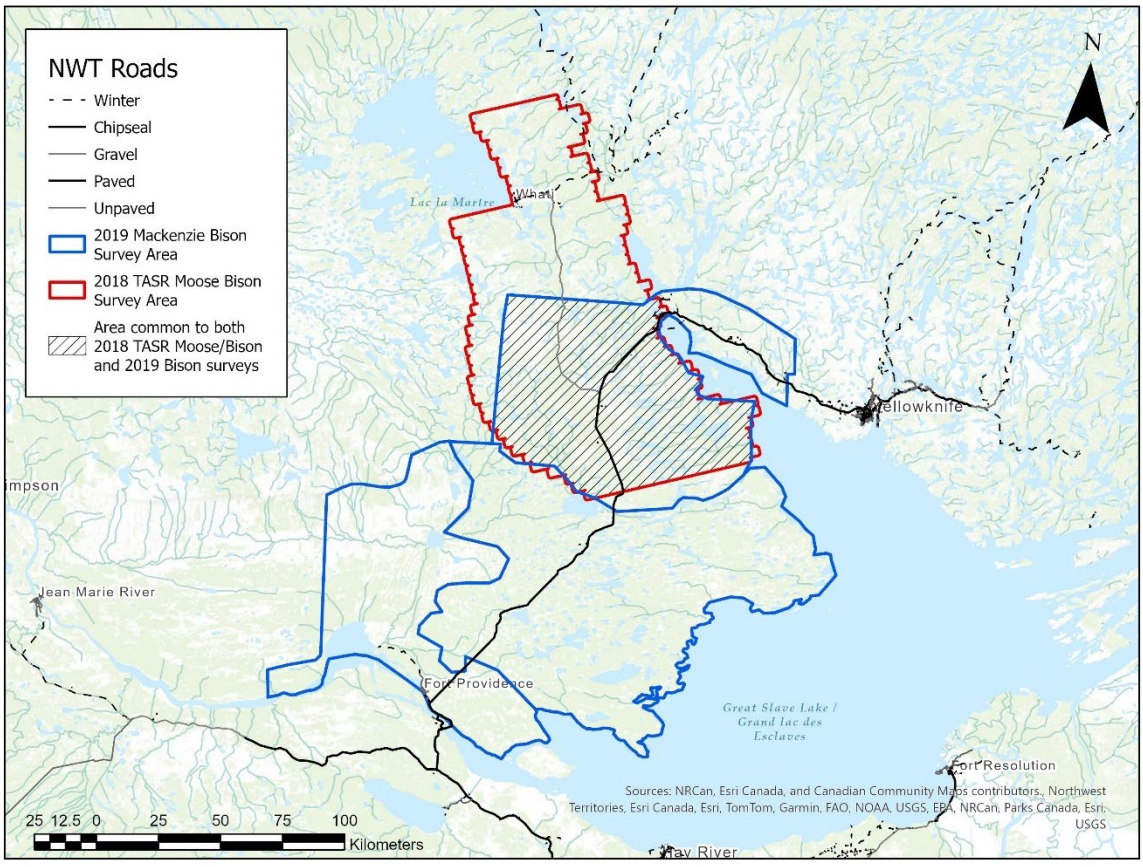

Figure D-11. Area for which 2018 bison density in the Tłı̨chǫ ASR survey area was estimated using bison abundance surveys. This area is the southern extent of the Tłı̨chǫ ASR survey area, where it overlaps with the 2019 Mackenzie bison survey extent.

Moose

Data Screening

Data from the Tłı̨chǫ ASR (TASR) sub-area of the 2021 NSR moose survey (Figure D-12) and the 2019 Mackenzie bison and moose survey (Figure D-13) were used to supplement the 2018 Tłı̨chǫ ASR moose survey. The Tłı̨chǫ ASR (TASR) sub-area of the 2021 NSR survey overlapped the 2018 Tłı̨chǫ ASR survey area (Figure D-13).

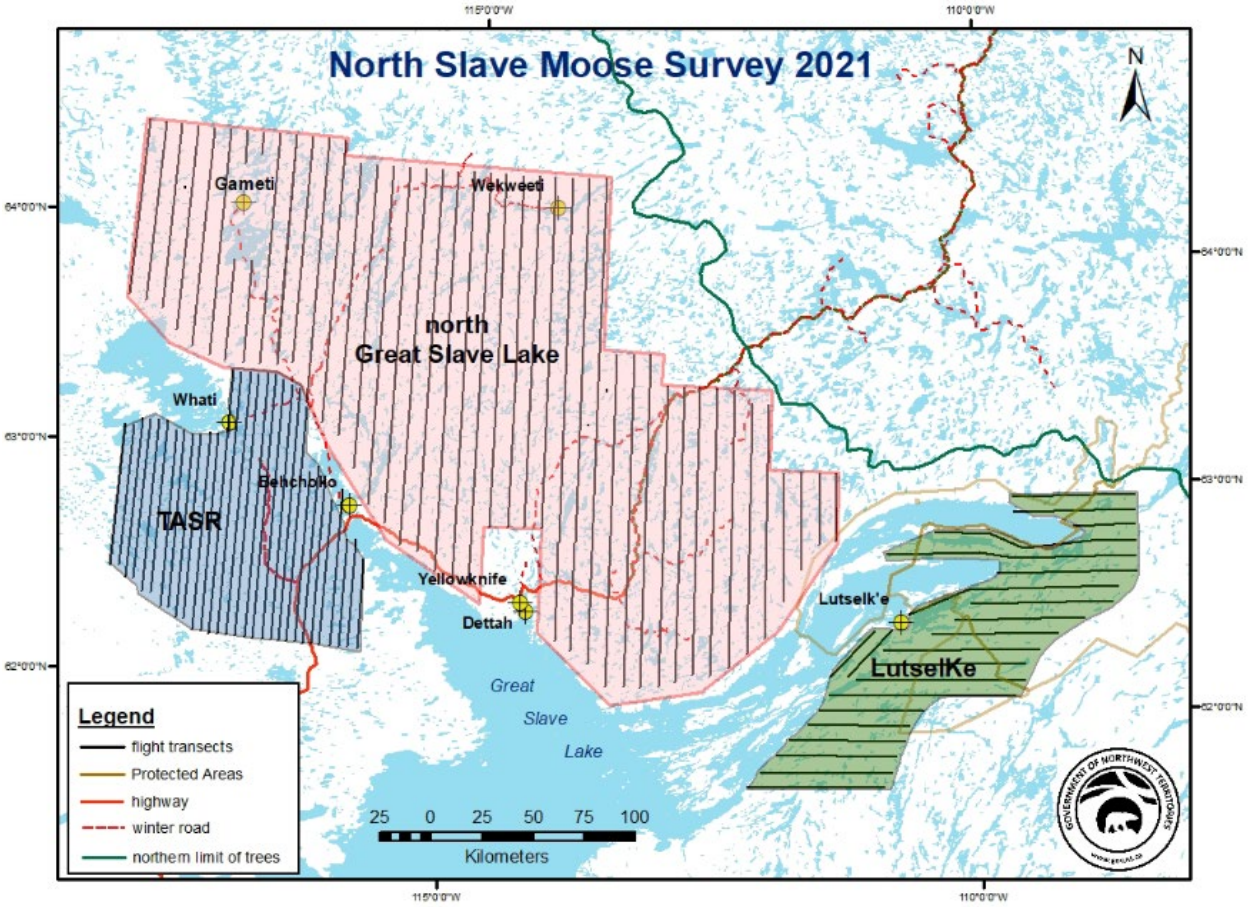

Figure D-12. 2021 North Slave moose survey sub-areas surveyed in March 2021. Moose observations from the Tłı̨chǫ ASR (TASR) sub-area shown in blue were used to supplement moose estimates from the 2018 Tłı̨chǫ ASR survey and to estimate moose abundance in 2018 and 2021.

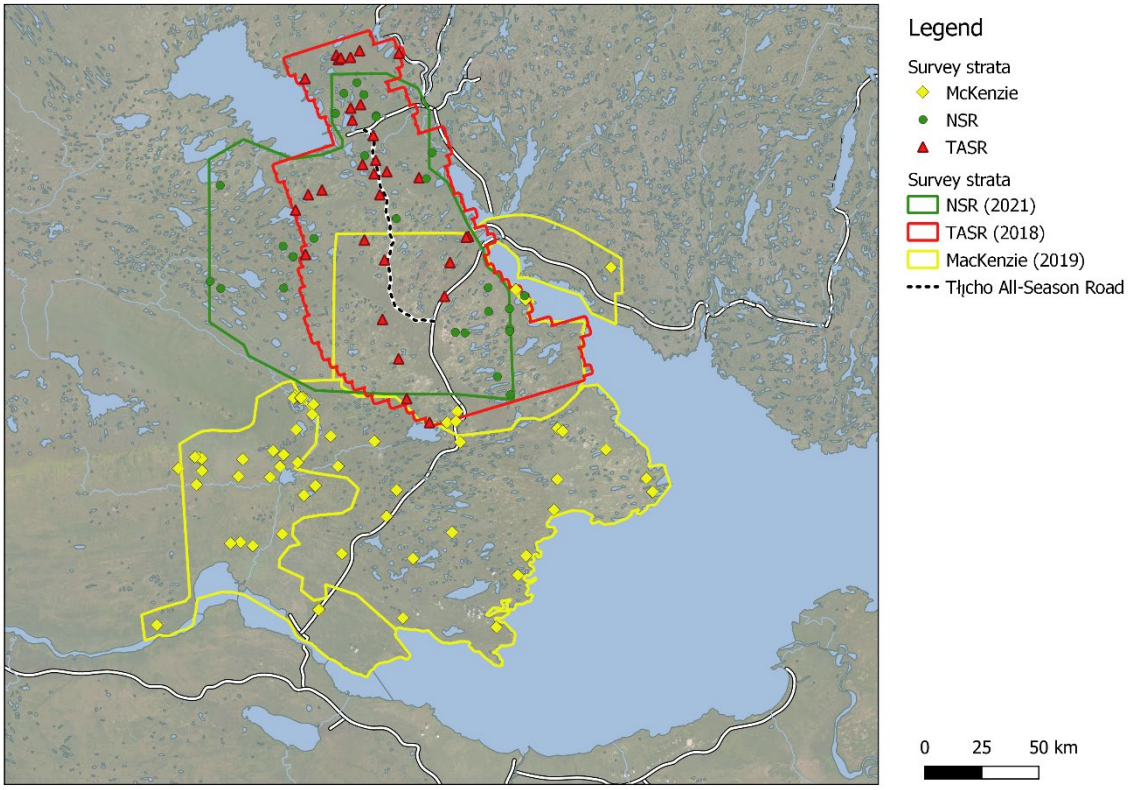

Figure D-13. Survey areas and moose observations for the Tłı̨chǫ ASR, NSR, and Mackenzie moose surveys.

Inspection of detection histograms revealed a blind spot near the plane as indicated by lower frequencies in the 0-200 m bin for the Mackenzie and Tłı̨chǫ ASR survey areas (Figure D-14). Observations at less than 200 m were left truncated to meet the assumption of perfect sightability near the plane. In contrast, the NSR survey used a Found Bush Hawk survey plane, which has a unique window configuration and did not have a noticeable blind-spot near the plane with the highest frequency of observations near the plane (Figure D-14). Left truncating this dataset would eliminate a substantial number of observations, therefore, the NSR dataset was not left truncated. In addition, the dataset was right truncated at 1,400 m, which eliminated some of the further Mackenzie survey observations.

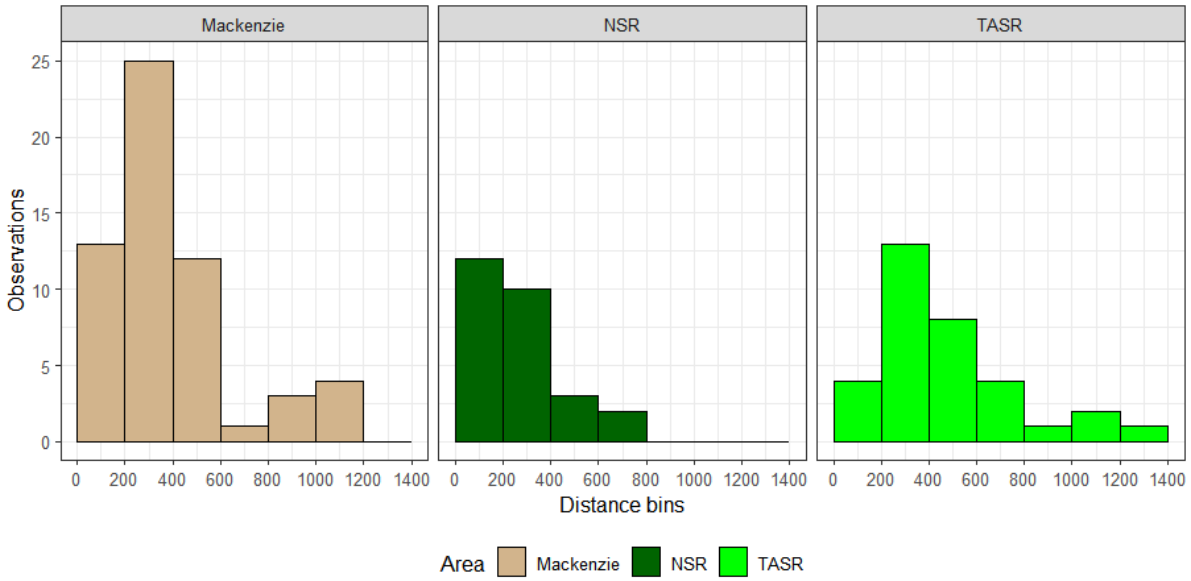

Figure D-14. Detection histograms for moose for each survey area before right and left truncation.

Figures D-15 and D-16 show the datasets with left and right truncation. The resulting histograms were similar in shape with a steady decline in sighting frequencies with distance from the plane.

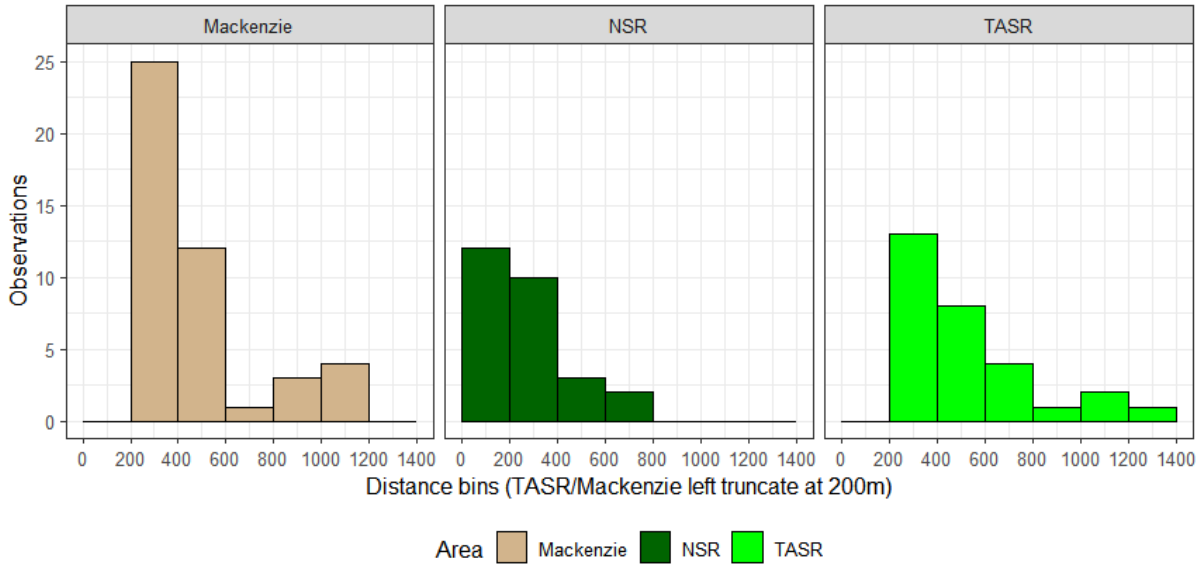

Figure D-15. Detection histograms demonstrating left truncation distances for Mackenzie and Tłı̨chǫ ASR.

Figure D-16 shows the combined detection histogram at 100 m bin intervals. For this diagram, 200 was subtracted from distances for Tłı̨chǫ ASR and Mackenzie.

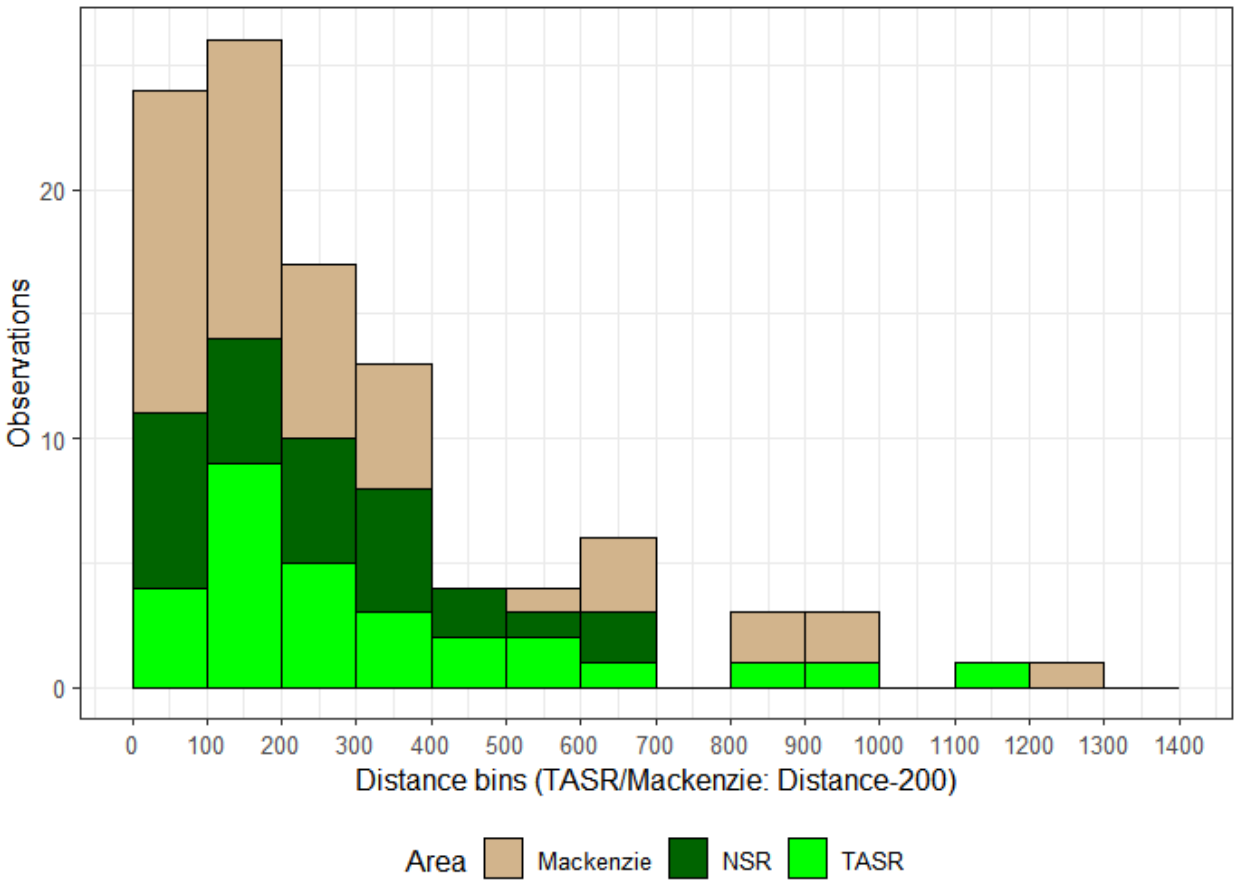

Figure D-16. Detection histogram for all areas.

Table D-5 summarizes observations of moose for each area. Overall, there were 102 groups with a total of 146 moose in the analysis.

Table D-5. Summary of moose observations used in the distance sampling analysis. Mackenzie and Tłı̨chǫ ASR were left-truncated at 200 m. All areas were right truncated at 1,400 m.

Area	Left-truncated		Used		Group size				Right-truncated	
	Moose	Groups	Moose	Groups	Group size	SD	Min	Max	Moose	Groups
Mackenzie	18	13	63	46	1.4	0.7	1	4	2	1
NSR	0	0	38	27	1.4	0.58	1	3	0	0
Tłı̨chǫ ASR	7	4	45	29	1.5	0.6	1	3	0	0
Totals	25	17	146	102					2	1

A covariate of interest was canopy cover. Canopy cover was not recorded for the NSR survey. The general spread of observations was relatively similar across classes and the NSR survey area (where no cover class was recorded) (Figure D-17). Canopy cover was modelled with NSR set to intercept values, to allow some modelling of canopy cover while including the NSR dataset.

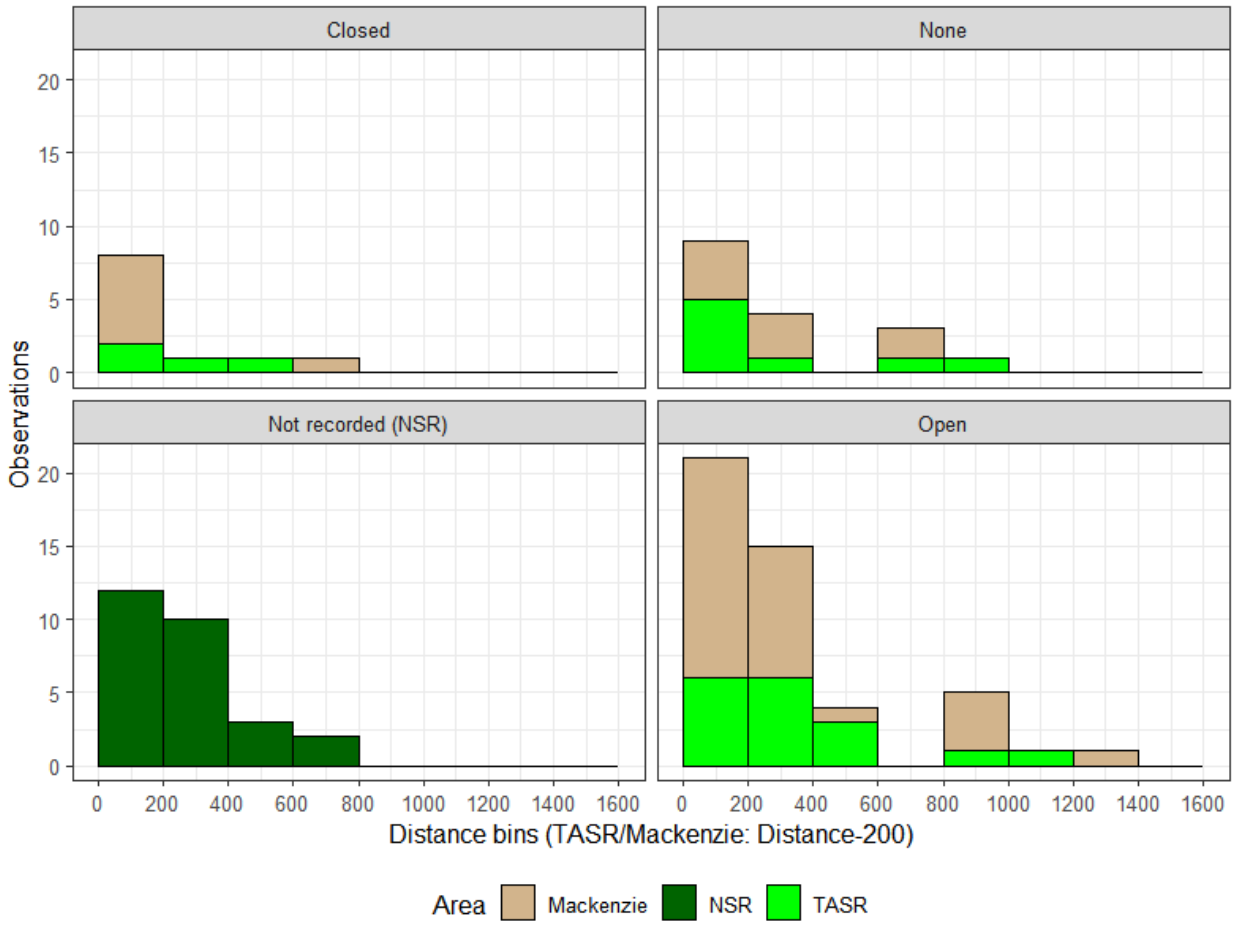

Figure D-17. Canopy cover class detection histograms with survey area delineated by sub-bars.

Counts of moose ranged from 1 to 4 with relatively little difference in detection histograms across count classes (Figure D-18).

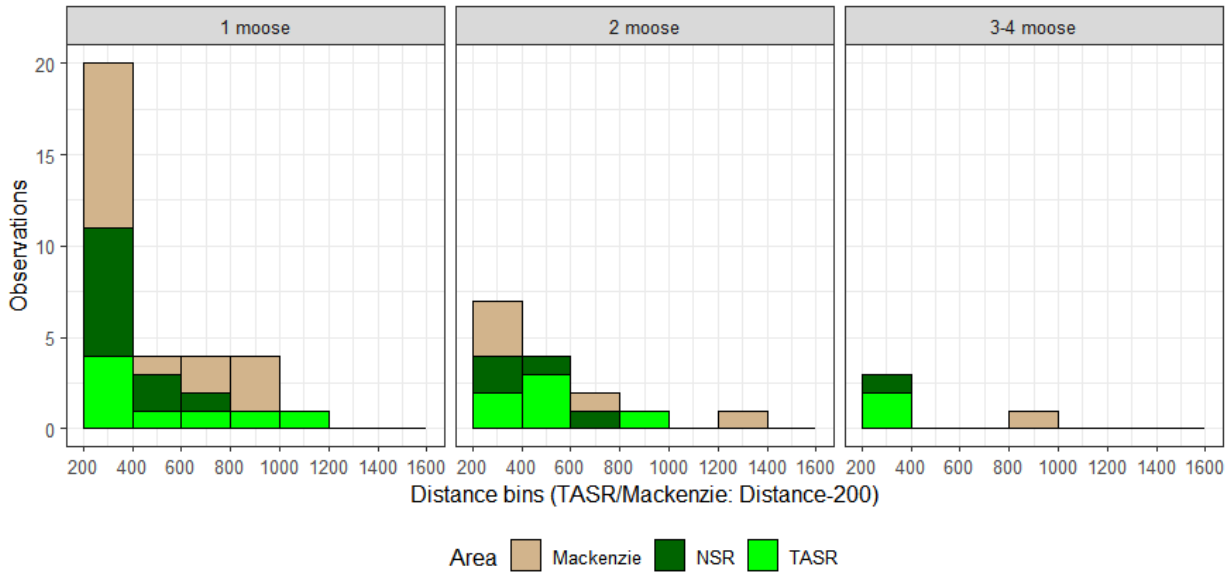

Figure D-18. Detection histograms as a function of group size classes.

Model Selection

Covariates considered in distance covariate models for moose included group size, canopy cover, and survey area (i.e., which survey the observations were from) (Figures D-13 to D-18). In addition, an NSR covariate, which contrasted detection function shape of the NSR survey with the other surveys (Mackenzie and TASR) was considered. Model selection results indicated that a hazard-rate detection function with no covariates was most supported (Table D-6). Unlike the bison analysis, only the hazard rate model was supported by the data as indicated by no other models that had a delta AICc value of two or less. The NSR survey (with no left truncation) did not have a detectable effect on the detection function despite the different survey methods employed. Estimates of abundance (for Tłı̨chǫ ASR and NSR combined) were generated for each model to assess the sensitivity of abundance estimates to model formulations. In general, estimates were not greatly affected by model formulation with differences of 10 or less moose in the most supported models.

Table D-6. Model selection of distance covariate models for moose. Base detection functions (DF) are given for each model; 'hn' and 'hr' symbolize half-normal and hazard rate detection function models with 0 adjustment terms. 'Size' refers to group size, 'area' refers to survey area, 'NSR' refers NSR survey (compared to the other surveys). AIC_c, the difference in AIC_c values between the ith model and the model with the lowest AIC_c value (ΔAICc), Akaike weights (w_i), number of parameters (K), and log-likelihood of the model are presented. Combined estimates for Tłı̨chǫ ASR and NSR are given (N) to assess sensitivity of estimates to model formulations.

DF	Model	AICc	ΔAICc	w_i	K	LogL	N	CV
hr	Constant	1,360.15	0.00	0.49	2	-678.0	295	0.22
hr	Size	1,362.18	2.03	0.18	3	-678.0	300	0.22
hr	NSR	1,362.27	2.12	0.17	3	-678.0	296	0.23
hr	Area	1,363.96	3.82	0.07	4	-677.8	285	0.24
hr	Canopy	1,364.69	4.54	0.05	5	-677.0	295	0.23

hn	NSR	1,366.95	6.80	0.02	2	-681.4	277	0.22
hn	Canopy	1,367.15	7.00	0.01	4	-679.4	281	0.22
hn	Constant	1,367.97	7.83	0.01	1	-683.0	243	0.19
hn	Area	1,368.99	8.85	0.01	3	-681.4	274	0.23
hn	Size	1,370.05	9.91	0.00	2	-683.0	244	0.19

The constant hazard rate model fit the data adequately as indicated by chi-square tests ($\chi^2 = 8.09$, df = 7, p = 0.32) and Cramer-von Mises tests (test = 0.19, p = 0.99). A plot of the dataset also suggests reasonable fit (Figure D-19).

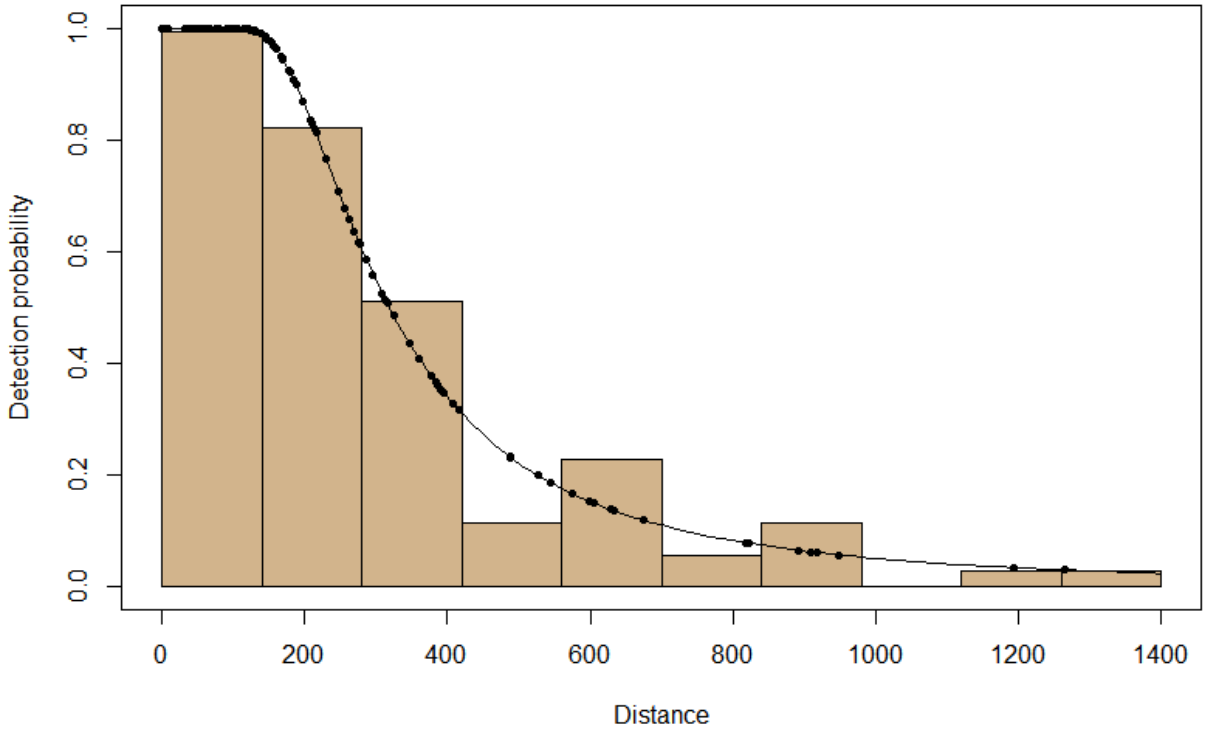

Figure D-19. Fit of constant hazard rate detection function to the moose dataset.

Estimates derived from the constant hazard rate model were of moderate precision with CVs of 0.25-0.28. The proportion of variance created by estimation of detection probabilities was 34% in contrast to 66% being due to encounter rate variation. Similar to bison, this suggests that the main source of variation was the unequal distribution of moose in the survey area.

The 2018 moose abundance estimate for the Tłı̨chǫ ASR area (11,005 km^2, shown in red in Figure D-13) was 113 moose (SE = 28.7, CI = 69-185, CV = 0.25). The estimated density of moose across the 2018 survey area was 1.03 moose / 100 km^2 (SE = 0.26, CI= 0.63-1.70) (Table D-7).

The 2021 moose abundance estimate for the Tłı̨chǫ ASR (TASR) sub-area of the North Slave moose survey (shown in green in Figure D-13) was 183 moose (SE = 50.6, CI = 106-316, CV = 0.28). The

estimated density of moose across the 11,830 km^2 survey area was 1.55 moose / 100 km^2 (SE = 0.43, CI= 0.89-2.67) (Table D-7).

The 2018 and 2021 survey extents had considerable overlap but were not the same (see Figure D-13). The best metric to compare estimates is density, which is not affected by survey extent. In this case density was higher in 2021, however, the confidence limits of each estimate overlapped point estimates of each year and therefore the differences were not statistically significant.

Table D-7. Estimates of moose abundance and density for the Tłı̨chǫ ASR (TASR) sub-area of the NSR survey (2021) and Tłı̨chǫ ASR study area (2018) from the constant hazard rate distance model.

Strata (year surveyed)	Survey area (km^2)	Groups	Individuals	Abundance					Density			
				N	SE	Conf. limit		CV	D	SE	Conf. limit	
NSR-TASR (2021)	11,830	25	35	183	50.6	106	316	0.28	1.55	0.43	0.89	2.67
Tłı̨chǫ ASR (2018)	11,005	29	45	113	28.7	69	185	0.25	1.03	0.26	0.63	1.70

Sensitivity Analyses

A series of sensitivity analyses were conducted to assess the robustness of moose estimates to analysis assumptions. First, the analysis involved left truncating the Mackenzie and Tłı̨chǫ ASR data sets at 200 m while not left truncating the NSR dataset. This approach assumes that sightability of moose at 200 m for Tłı̨chǫ ASR/Mackenzie is similar to sightability on the line for the NSR survey. As a test of sensitivity, the most supported hazard rate model was run with the NSR data excluded from the dataset to test if inclusion of NSR with a different truncation distance affected Tłı̨chǫ ASR estimates. A left truncation distance of 200 m was still used with the Mackenzie and Tłı̨chǫ ASR datasets for the analysis. The resulting estimate for Tłı̨chǫ ASR was 120.4 (SE = 37.1, CI = 66-219, CV = 0.31) from the constant hazard rate model suggesting that the variable truncation distance approach used had minimal effect on Tłı̨chǫ ASR estimates (beyond a slight increase in precision with the combined dataset). The NSR dataset was then run as a standalone dataset with a right truncation distance set to 700 m, which was the range of the observed data (with no left truncation distance). The resulting estimate for NSR was 184 (SE = 68.7, CI = 89-378, CV = 0.37), which was similar to the combined analysis except the estimate was much less precise. In conclusion, combining the datasets provided an efficient method for the analysis (increasing precision) with minimal change in estimates compared to stand-alone analyses.

More aggressive left truncation distances were then applied to the full dataset with relatively little effect on the estimates, suggesting that blind spot areas did not extend beyond the left truncation used (Figure D-20).

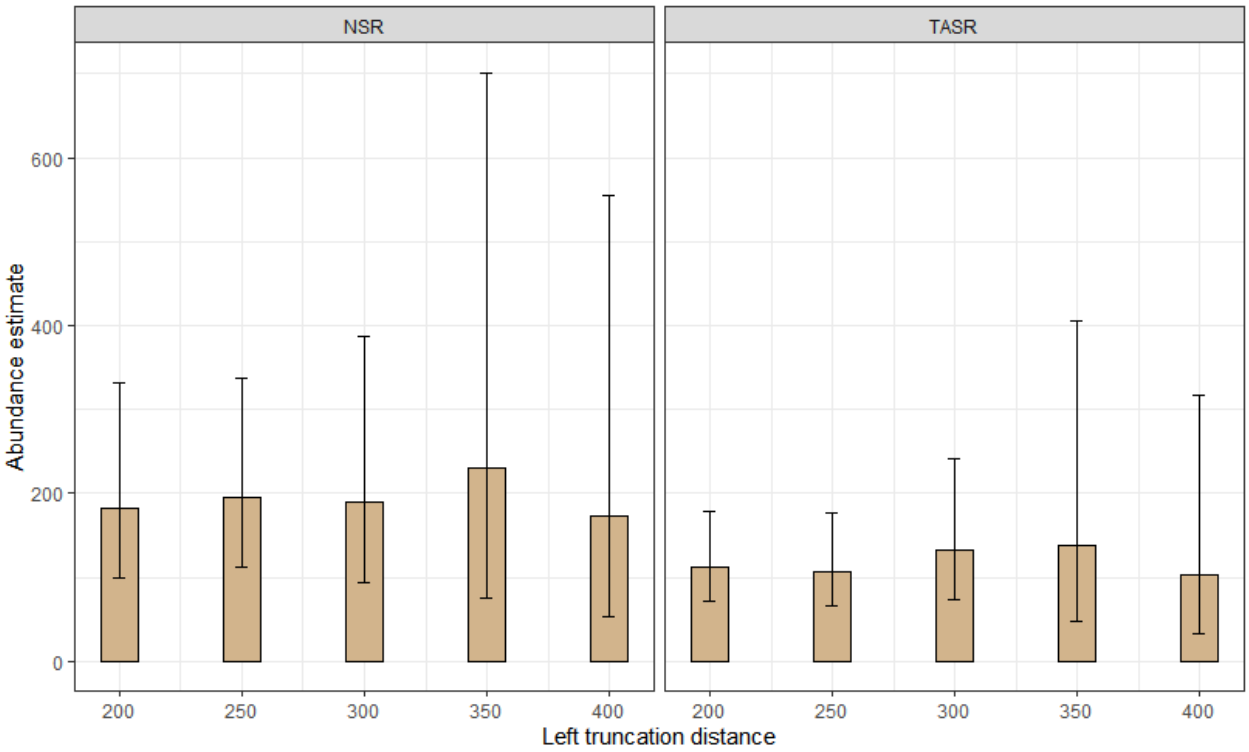

Figure D-20. Sensitivity of moose abundance estimates to left truncation distances. The 200 m distance is what was used in the analysis for Tłı̨chǫ ASR and ASR/Mackenzie.

Estimates were also run for decreasing right truncation distances with minimal sensitivity in estimates (Figure D-21).

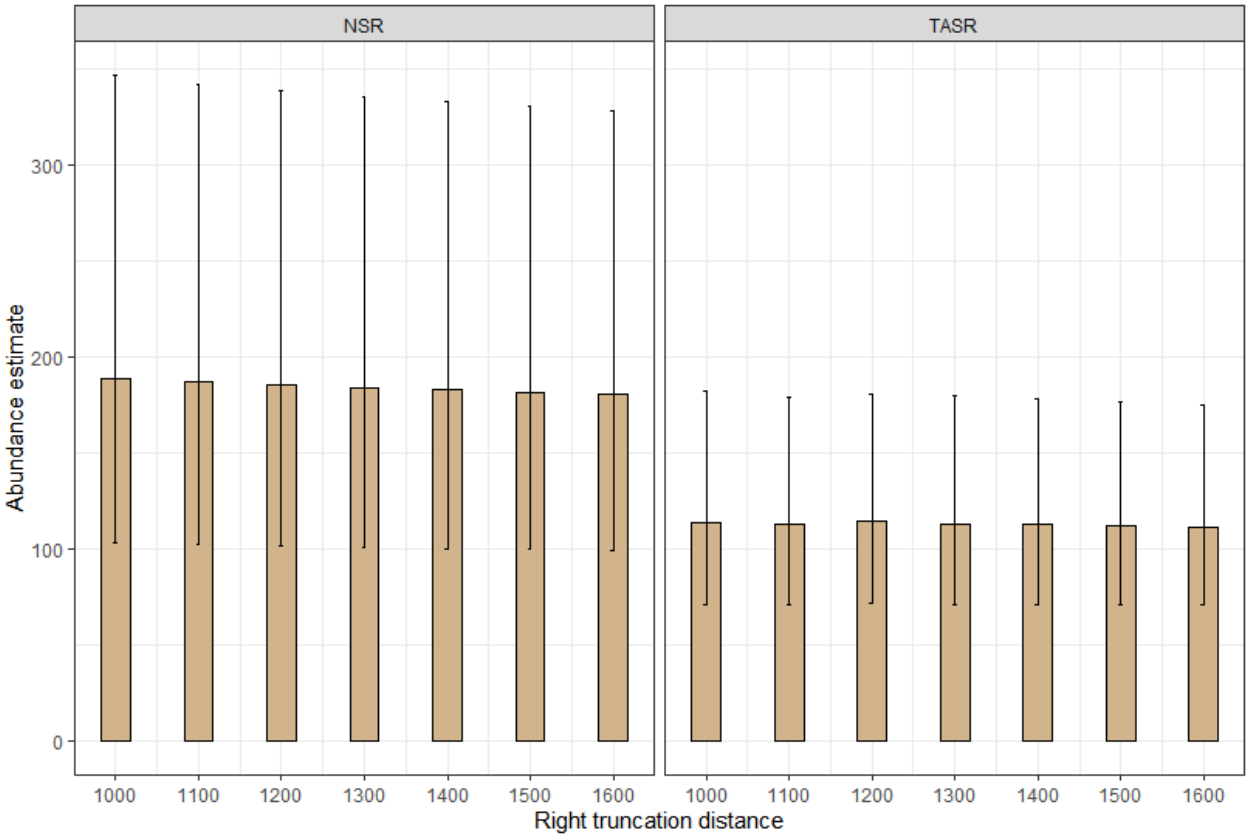

Figure D-21. Sensitivity of moose abundance estimates to right truncation distances.

Discussion

Bison

Although the 2018 survey covered the full extent of the Tłı̨chǫ ASR alignment, bison were only observed in the southern part of the survey area. Compared to using the full 2018 Tłı̨chǫ ASR survey extent, estimates were similar if only the southern area was used for the analysis given that a systematic random survey design was used. Precision of estimates was also similar using a reduced study area. The model averaged estimate of 197 bison (SE = 79.2, CI = 91-423, CV = 40%) is the most robust estimate in that it considers model selection uncertainty. The precision of estimates, as indicated by coefficient of variation, for the Tłı̨chǫ ASR survey were similar to that of the north strata of previous Mackenzie bison surveys, which have ranged from 0.33-0.60 (GNWT-ECC unpublished data)

The main factor limiting precision of bison surveys is the aggregated distribution of groups, which leads to a large degree of variation in encounter rate (which is basically variation in transect densities). Density surface modelling (Miller et al. 2013, 2016) is an approach to confront aggregation as well as learn more about factors influencing density. For example, this approach could be used to assess if density changes as a function of distance from the road in successive surveys. This approach was applied to the Slave River 2016 bison data set (Boulanger 2017) with improvements in precision.

Moose

Estimates of moose had moderate precision, which was due primarily to variation in encounter rates caused by variation in moose densities across the study area.

The main assumption of moose abundance distance models was that sighting probability at the 200 m left truncation distance was equal to 1. If it was less than 1 then estimates will display a negative bias. In terms of this analysis, comparison of estimates from the 2021 NSR and 2018 Tłı̨chǫ ASR survey involves the assumption of similar sightability of moose on the survey line in each survey. The 2021 NSR survey used a Bush Hawk plane that did not have a noticeable blind spot compared to aircraft used for the 2019 Mackenzie and 2018 Tłı̨chǫ ASR surveys. Also, the range of distances of detection were less than the Tłı̨chǫ ASR/Mackenzie surveys suggesting more observer attention to areas closer to the plane. This method may have increased sightability on the line compared to the Tłı̨chǫ ASR/Mackenzie surveys. Left truncating the Tłı̨chǫ ASR and Mackenzie data helped meet this assumption by eliminating the likely blind spot under the plane where moose could not be observed. However, in this case the assumption is that moose at 200 m from the plane in the Tłı̨chǫ ASR/Mackenzie surveys will be similar to moose sightability under the NSR plane. For example, a difference in estimates could arise if sightability under the plane was close to 1 for NSR but less than 1 at 200 m for the Tłı̨chǫ ASR and ASR/Mackenzie surveys.

The NSR and Tłı̨chǫ ASR/Mackenzie surveys were run in a single analysis under the assumption that the detection histograms and resulting detection functions were similar between surveys. A model with NSR as a covariate was not supported in the detection function analysis suggesting this was a reasonable assumption. In addition, sensitivity analyses where the Tłı̨chǫ ASR/Mackenzie and NSR were run as stand-alone analyses showed little change in estimates, with reduced precision. Results suggested that combining the datasets for the analysis did not substantially affect estimates but did lead to estimates with higher precision especially for the NSR survey.

In review, the main assumption with distance surveys is that sightability is close to 1 on the survey line. Methods are available to further assess this assumption. Use of double observer methods could estimate detection probability at the line if the probability of sighting is reasonable (>0.5) (Laake et al. 2008). If moose are in thick cover so that sighting probability is substantially less than 1 then the use of sightability models in unison with distance sampling is the best approach to ensure robust estimates of abundance (Peters et al. 2014).

Approach for Future Surveys

The low number of bison and moose observations during the 2018 Tłı̨chǫ ASR survey required combining the 2018 survey data with bison and moose observations from other distance sampling surveys to obtain abundance estimates. In a 2019 review of the wildlife effects monitoring programs in the WMMP for the Tłı̨chǫ ASR, it was recommended that future aerial surveys for moose and bison for the Tłı̨chǫ ASR be combined with the larger regional North Slave moose aerial survey, and the Mackenzie bison population surveys, both of which use a distance-based sampling approach (Rettie 2019). Combining the Tłı̨chǫ ASR survey with the broader regional surveys should provide the necessary number of observations to reliably estimate detection functions, and to generate

population estimates with an improved level of precision for both species. The Tłı̨chǫ ASR study area will be treated as a stratum within the broader regional moose and bison population survey areas in order to estimate moose and bison densities specific to this area.

References

Appelhans, T., Detsch, F., Reudenbach, C., and Woellauer, S. 2023. mapview: interactive viewing of spatial data R package version 2.11.0.9006. Available online: https://github.com/r-spatial/mapview.

Boulanger, J. 2017. Estimates of population size and factors influencing density for the 2016 Slave River Lowlands bison survey. Department of Environment and Natural Resources, Government of the Northwest Territories, Yellowknife, NT.

Buckland, S.T., Anderson, D.R., Burnham, K.P., and Laake, J.L. 1993. Distance Sampling: Estimating Abundance of Biological Populations. Chapman & Hall, London, UK.

Buckland, S.T., Anderson, D.R., Burnham, K.P., Laake, J.L., Borchers, D.L. and Thomas, L., 2001. Introduction to distance sampling: estimating abundance of biological populations. Oxford university press.

Buckland, S.T., Anderson, D.R., Burnham, K.P., Laake, J.L., Borchers, D.L., and Thomas, L. 2004. Advanced distance sampling - estimating abundance of biological populations. Oxford Press, Oxford, UK.

Burnham, K.P. and Anderson, D.R. 1992. Data-based selection of the appropriate model: the key to modern data analysis. Pages 16-30 *In:* McCullough, D.R. and Barrett, R. Eds. Wildlife 2001: Populations. Elsevier, New York, USA.

Hodson, J. and Patenaude, A. 2018. Summary of winter 2018 field work carried out under wildlife research permit WL5005580 – "Wildlife effects monitoring for the proposed Tłı̨chǫ all-season road". Department of Environment and Natural Resources, Government of the Northwest Territories, Yellowknife, NT.

Innes, S., Heidi-Jorgensen, M.P., Laake, J.L., Laidre, K.L., Cleator, H.J., Richard, P., and Stewart, R.E.A. 2002. Surveys of belugas and narwhals in the Canadian high arctic. NAMMMCO Scientific Publications, 4: 169-190.

Laake, J., Borchers, D.L., Thomas, L., Miller, D., and Bishop, J. 2012. Mark-recapture distance sampling (MRDS) 2.1.0. R statistical package program. Available online: https://cran.r-project.org/web/packages/mrds/index.html.

Laake, J., Dawson, M.J., and Hone, J. 2008. Visibility bias in aerial survey: mark-recapture, line-transect or both? Wildlife Research, 35: 299-309.

Miller, D.L., Burt, M.L., Rexstad, E.A., and Thomas, L. 2013. Spatial models for distance sampling data: recent developments and future directions. Methods in Ecology and Evolution, 4: 1001-1010.

Miller, D.L., Rexstad, E., Burt, L., Bravington, M.V., and Hedley, S.L. 2016. Package DSM: density surface modelling of distance sampling data, version 2.2.13. Available online: https://www.google.com/url?sa=t&source=web&rct=j&opi=89978449&url=https://cran.r-project.org/web/packages/dsm/dsm.pdf&ved=2ahUKEwigrpngvLqOAxVtJEQIHY0LAU8QjJEMegQIAxAB&usg=AOvVaw3SIzsqBiAxPHCu5-wascEr.

Pebesma, E. 2018. Simple features for R: standardized support for spatial vector data. The R Journal, 10: 439-446.

Peters, W., Hebblewhite, M., Smith, K.G., Webb, S.M., Webb, N., Russell, M., Stambaugh, C., and Anderson, R.B. 2014. Contrasting aerial moose population estimation methods and evaluating sightability in west-central Alberta, Canada. Wildlife Society Bulletin, 38: 639-649.

QGIS Foundation. 2020. QGIS Geographic Information System. QGIS Association. Available online: http://www.qgis.org.

R Development Core Team. 2023. R foundation for statistical computing. Vienna, Austria.

Rettie, W.J. 2019. Review of wildlife effects monitoring programs in the Wildlife Management and Monitoring Plan for the Tłı̨chǫ All-Season Road. Report prepared for Government of the Northwest Territories, Department of Environment and Natural Resources by Paragon Wildlife Research and Analysis Ltd. 39 pp.

Thomas, D.C., Buckland, S.T., Rexstad, E.A., Laake, J., Strindberg, S., Hedley, S.L., Bishop, J.R.B., Marques, T.A., and Burnham, K.P. 2009. Distance software: sesign and analysis of distance sampling surveys for estimating population size. Journal of Applied Ecology, 47: 5-14.

Wickham, H. 2009. ggplot2: elegant graphics for data analysis. Springer, New York.